one can estimate $c \sin \beta^*$ using eq A3. One can then calculate the values of β^*, and thus c, for different possible l values using eq A2. We have attempted to elucidate the crystal structure by first refining against contact constraints alone so as to minimize contacts between the side chains and from there to refine the headgroup packing using the electron diffraction data. This was done for all reasonable values of D_c, c, β^*, and l.

Registry No. $DC_{8,9}PC$, 109150-63-2.

Formation of Graphite Flakes from Aromatic Precursors: A Comparison of Benzene- and Triphenylene-Derived Graphites

Dong Pyo Kim and M. M. Labes*

Department of Chemistry, Temple University, Philadelphia, Pennsylvania 19122

Received April 4, 1990

The formation of graphite flakes from the decomposition of the aromatic precursors benzene and triphenylene is studied in detail. X-ray diffraction, Raman spectroscopy, scanning electron microscopy, and conductivity measurements are reported as a function of heat treatment temperatures. Benzene appears to form an ideal size nucleus, leading to high-quality oriented graphite, whereas triphenylene-derived graphites are more disordered and undergo exfoliation in the high-temperature annealing process.

Introduction

Carbons that are, at least in part, sp^2 hybridized can be produced in discrete morphological forms by thermal decomposition of precursor fibers or films in a controlled manner. Primary examples of these processes are the preparation of carbon fibers by the decomposition of poly(acrylonitrile) (PAN)[1] or the decomposition of pitch fibers that have been extruded from the mesophase into fiber form.[2,3] Films of PAN[4] and other polymers[5,6] can also be decomposed to give coherent thin films of partially graphitized carbon on an appropriate substrate.

Vapor-phase decomposition of hydrocarbons can also be controlled to give discrete morphological entities under appropriate nucleation conditions. The vapor growth of short carbon fibers (essentially whiskers, VGCF) is based on the observations of the nucleation of carbon whisker growth on fine metal particles. A brief review by Tibbetts of the status of vapor-grown carbon fibers (VGCF) has recently appeared.[7] Koyama and Endo[8] patented a process for producing carbon filaments and fibers by having fine metal particles mix with a hydrocarbon gas near the inlet of a furnace. These filaments consist of nested, rolled-up basal planes of graphite, with a hollow core.[9] Tibbetts[7] proposes a model in which carbon atoms diffuse through the bulk of the metal catalytic particle and precipitate in a graphitic layer growing from the surface of the catalytic particle. These layers are then thickened by vapor-phase deposition of carbon on the exterior surface. Although there is promise to this method, it has not been developed beyond the small-batch noncontinuous fiber production stage. Nevertheless, VGCF fibers have superior thermal and electrical conductivity as compared to PAN-based fibers and are about equal to pitch-based fibers in these properties.

Several vapor decomposition pathways to films have been reported,[10,11] such as the decomposition of 3,4,9,10-perylenetetracarboxylic dianhydride (PTCDA), conducted at 700–900 °C in vacuum.[12] The thickness of the resultant poly(perinaphthalene) (PPN) films varied from several hundred angstroms to approximately 1 μm. Formation of PPN fibers and ribbonlike PPN has also been reported by several groups.[13,14]

In our recent work,[15] we have found conditions under which simple aromatic hydrocarbons and heterocycles can be efficiently converted to highly conducting flakes in a practical and inexpensive manner. Although there is extensive literature dealing with preparation of carbons from such precursors, the morphological characteristics—well-formed flakes—observed in this work are atypical. The approach involves the pyrolysis of hydrocarbon at 800 °C in the presence of halogen vapor. These flakes have a metallic luster and high electrical conductivity and are chemically inert and thermally stable. The starting materials are simple and inexpensive, and the yields of gra-

(1) Donnet, J. B.; Bansal, R. C. *Comprehensive Polymer Science*; Pergamon Press: Oxford, 1989; Vol. 7, p 501.
(2) Lewis, I. C.; Singer, L. S. *Adv. Chem. Ser.* **1988**, 217, 269.
(3) Daumit, G. P. *Carbon* **1989**, *27*, 759.
(4) Renschler, C. L.; Sylwester, A. P.; Salgado, L. V. *J. Mater. Res.* **1989**, *4*, 452.
(5) Ohnishi, T.; Murase, I.; Noguchi, K. *Synth. Met.* **1986**, *14*, 207.
(6) Murakami, M.; Yoshimura, S. *Synth. Met.* **1987**, *18*, 509.
(7) Tibbetts, G. G. *Carbon* **1989**, *27*, 745.
(8) Koyama, T.; Endo, M. Japanese Patent No. 58966, 1982.
(9) Tibbetts, G. G.; Endo, M.; Beetz, C. P. *SAMPE J.* **1986**, *22*, 30.
(10) Fitzer, E.; Mueller, K. *Chemistry and Physics of Carbon*; Marcel Dekker: New York, 1971; Vol. 7, p 237.
(11) Chiang, L. Y.; Stokes, J. P.; Johnston, D.C.; Goshorn, D. P. *Synth. Met.* **1989**, *29*, E483.
(12) Kaplan, M. L.; Schmidt, P. H.; Chen, C.; Walsh, W. M. *Appl. Phys. Lett.* **1980**, *36*, 867.
(13) Iqbal, A.; Ivory, D. M.; Marti, J.; Baughman, R. H. *Mol. Cryst. Liq. Cryst.* **1985**, *118*, 103.
(14) Murakami, M. *Synth. Met.* **1987**, *18*, 531.
(15) Chang, P. H.; Labes, M. M. *Chem. Mater.* **1989**, *1*, 523.

0897-4756/90/2802-0599$02.50/0

phitic material are relatively high.

In this paper, we wish to report a detailed study of the differences in the properties of these graphites as a function of aromatic precursor and postpreparation heat treatment. We believe the ease of formation of graphite flakes from vapor sources on a quartz surface affords an opportunity to explore structure–property relationships and mechanisms of graphitization. As the first stage of this exploration, we elected to study two aromatic precursors whose mechanistic pathways to graphite would of necessity be quite different: benzene (B) and triphenylene (TP). In both cases, we obtain well-formed flakes of thicknesses up to 20 μm and lengths up to 10 cm on a side. The flakes are then annealed at various heat-treatment temperatures (HTT) to improve graphitic order, and X-ray, Raman spectroscopy, scanning electron microscopy, conductivity, density, and electron spin resonance measurements are performed to fully characterize the materials.

Experimental Section

Benzene (B), biphenyl (BP), bromobenzene (BrB), *o*-terphenyl (TER), and triphenylene (TP) were purchased from Aldrich and used as received. Pyrolysis was carried out under carefully controlled conditions, maintaining a uniform size quartz tube (38-mm diameter × 18-in. hot zone), an argon carrier gas flow rate of 15 cm^3/min, and a temperature of 800 °C. Chlorine vapor was introduced in trace amounts into the argon carrier gas stream. The role of chlorine is to promote dehydrogenation by first substituting for hydrogen and then being eliminated as HCl.[16] During this process, however, the overall rate of radical formation is enhanced. Samples have some residual chlorine (1–2%) when prepared at 800 °C; this chlorine is completely eliminated at 1000 °C. B was purged into the hot zone by bubbling carrier gas into the liquid heated to 50 °C (vapor pressure 270 mmHg). TP powder was placed in an inlet adaptor heated to 300 °C to also provide a vapor pressure of 270 mmHg.

Samples were removed from the quartz tube to allow heating to higher temperatures. Graphitization of samples was performed in a high-temperture furnace (Thermal Technology's Group 1000) that was fitted with a graphite hearth. The samples were placed in a graphite crucible and heated in a helium atmosphere for periods of 5 min to 4 days at a heat-treatment temperature (HTT) of 1200–2600 °C. Samples were heated by two different protocols: (1) rapid ($^1/_2$ h) approximately linear heating to each HTT; (2) 1-h linear heating to 1200 °C, followed by a 1-h anneal at that temperature, followed by slowly heating (~1 h) to the final HTT, followed by a 1-h anneal.

X-ray diffraction (XRD) data were obtained on a Rigaku D/Max2 instrument, using Cu Kα radiation. Both powdered samples and film samples were attached to Kapton 3M no. 92 tape for XRD. Additional XRD determinations to measure the mosaic spread, $\Delta\delta_{fwhm(002)}$, using Mo Kα radiation were performed by Dr. Paul Heiney at the University of Pennsylvania. Conductivity was measured by a standard four-probe technique, attaching four gold or silver wires to the film (mounted on a thin insulating substrate) with silver paint (Du Pont 4922). The dimension of samples were measured by both optical microscopy and scanning electron microscopy (SEM). Photomicrographs of the surface morphology of the samples were also taken by using SEM. Raman spectroscopy utilizing the microprobe techniqe allowed for characterization of the degree of graphitic order of pyrolytic films. A Bruker ER200D-SRC electron spin resonance spectrometer (ESR) was used to measure the characteristics of fine powder samples in the temperature range 120–300 K.

Results and Discussion

The XRD pattern consists of only crystalline reflection (00*l*) lines, with the (002) lines always having the highest intensity. The layer thickness along the *c*-axis (L_c) is determined from the half-peak width of the (004) line by means of the Scherrer formula.[17] Owing to the poor resolution of the (002) line, *d* spacing and layer thickness are best determined from the (004) line; however, values obtained from the (002) lines are consistent with those obtained from (004).

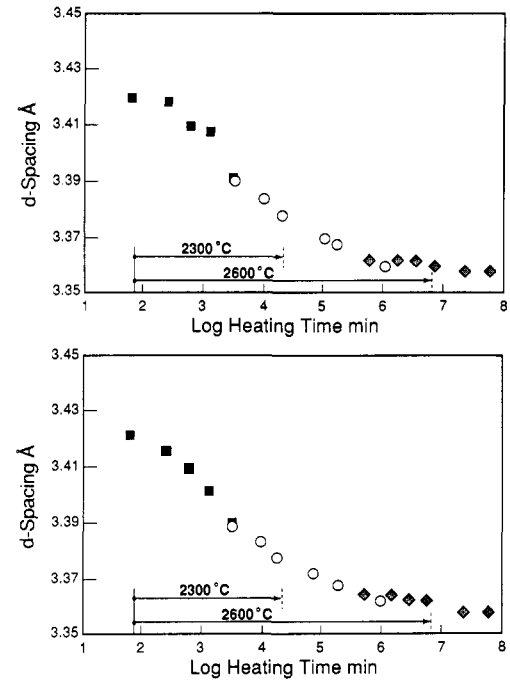

Figure 1. Dependence of lattice *d* spacing on heat treatment time at three heat treatment temperatures for benzene (upper) and triphenylene- (lower) derived graphites: ■, 2000 °C; ○, 2300 °C; ◆, 2600 °C. The latter two data sets are translated along the time axis (see text).

To show the dependence of *d* spacing on heat-treatment time, a composite curve is constructed of all data at the three HTTs of 2000, 2300, and 2600 °C by translating the latter two data sets along the time axis to allow them to superimpose smoothly on the former data set. Such a composite curve may be interpreted as representing the behavior that would have been observed at 2000 °C if treatment times could have been extended to ~10^6 min (about 2 years) and is an approach that has been used by Fischbach[18] in analyzing similar data. Figure 1 shows such a curve for both B and TP, and it can clearly be seen that the *d* spacing reaches graphitelike values at essentially the same rate in both systems. Both B- and TP-derived carbons show a transition from a poorly oriented state with a *d* spacing of 3.42 Å to an oriented state with a *d* spacing of 3.35 Å. L_c increases from 100 to 400 Å with increasing HTT in both materials, indicating grouping in parallel packets of from 30 to 120 layers, with no significant difference between B and TP.

The development of a graphitic structure—that is, the beginning of a preferred orientation of graphite planes is best judged from the appearance and intensity of the (002) line in the XRD. Virtually no diffraction is observed in 800 °C products, except in the cases of BrB and B, which show a trace of the (002) line. In Figure 2, data at a HTT of 1200 °C are presented for BrB, B, TP, TER, and BP. The quality of the diffraction patterns in Figure 2 is poor; they are shown simply to illustrate the first indications of graphitization.

(16) Stacy, W. O.; Walker, P. L. *Carbon* **1966**, *4*, 343.

(17) Bokros, A. W. *Chemistry and Pysics of Carbon*; Marcel Dekker: New York, 1969; Vol. 5, p 1.

(18) Fischbach, D. B. *Nature* **1963**, *200*, 1281.

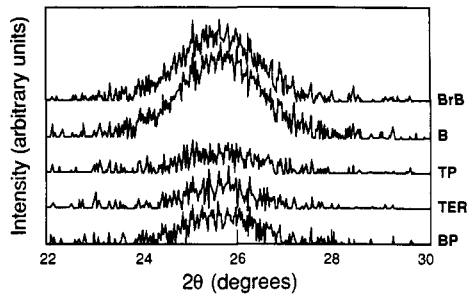

Figure 2. Intensity of the X-ray diffraction (002) line at the early stages of graphitization for five different hydrocarbon precursors heated at 1200 °C for two days. BP = biphenyl, TER = terphenyl, TP = triphenylene, B = benzene, BrB = bromobenzene.

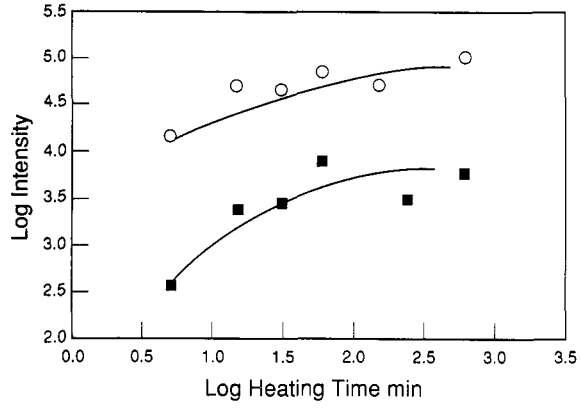

Figure 3. Intensity of the X-ray diffraction (002) line for benzene- (upper) and triphenylene- (lower) derived graphites as a function of heating time at 2600 °C.

Table I. Mosaic Spread of the Surfaces of B- and TP-Derived Graphites from an Intensity Scan vs θ (Incident Angle) at Fixed 2θ (Diffracted Angle)

sample	anneal temp, °C	$\Delta\delta_{fwhm(002)}$
B	2000	4.0
B	2600	7.5
TP	1500	16.5
TP	2000	11.0
TP	2600	80.0

The extent of orientation of the polycrystalline domains is indicated by the mosaic spread, $\Delta\delta_{fwhm(002)}$, defined as the full width at half-maximum intensity of the (002) line obtained from an intensity scan versus θ (incident angle) at fixed 2θ (diffracted angle). Table I shows the mosaic spread of samples as a function of HTT. For B, these values approach those of highly oriented pyrolytic graphite (HOPG), 0.5–5°.[19] For TP, the mosaic is wider than that of B and gets incredibly broad when exfoliation ocurrs during rapid heating at 2600 °C.

Figure 3 presents the (002) line intensity as measured in counts per second against heat treatment time at 2600 °C for both B and TP. B-derived samples uniformly show a higher peak intensity than TP-derived samples, with similar time dependences.

A significant difference is found in the conductivity of B and TP derived samples as shown in Figure 4. The conductivity of B-derived samples increases 40-fold comparing samples at HTTs of 2000 and 2600 °C, whereas TP-derived graphites show a constant conductivity as a function of HTT of 10^3 S cm^{-1}. The major reasons for these differences in conductivity are (a) the strong exfoliation seen in the TP samples and (b) the differences in microstructure of TP and B samples. Both these structural features can be seen clearly in SEM photographs shown in Figure 5. The differences in the in-plane conductivity starting at HTT 2300 °C in B- and TP-derived samples are due in part to the folded, wrinkled surface of films caused by exfoliation and also due to the beaded structures seen in TP-derived samples. It is known that, in intercalated graphites, exfoliation decreases the *a* axis conductivity due to the bending of the graphite layer.[20]

Figure 5 shows SEM photographs of B and TP surfaces. Surfaces of TP starting at 2000 °C show significant exfoliation, whereas B samples show only a trace of exfoliation at 2600 °C. Slow heat treatment can eliminate the exfoliation in B, leading to an extremely smooth surface even at 2600 °C; in the case of TP, even slow heating leads to significant surface damage. In slow heat treatment, one expects the slow release of hydrogen, which must be eliminated from the 800 °C carbons, as well as small amounts of methane, which may be trapped at defects during py-

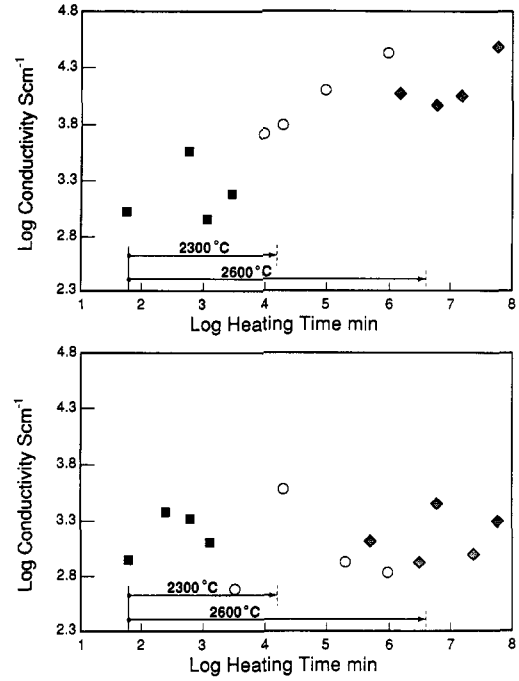

Figure 4. Conductivity vs heat treatment time at three different temperatures for benzene- (upper) and triphenylene- (lower) derived graphites: ■, 2000 °C; ○, 2300 °C; ◆, 2600 °C. The data at the upper two temperatures are translated along the time axis by indicated amounts to produce a smooth curve, which can be interpreted as effective heating time at 2000 °C.

Table II. Comparison of ESR Measurements on B- and TP-Derived Carbons Prepared at 800 °C

sample	temp, K	line width δH, G	spin density, spin g^{-1} × 10^{-18}
TP	120	2.81	4.97
TP	140	2.87	5.02
TP	180	2.98	5.50
TP	220	2.69	5.69
TP	260	2.84	5.99
TP	300	2.73	6.32
B	120	0.86	9.1
B	140	0.82	12.2
B	180	0.94	12.5
B	220	1.00	12.7
B	260	0.97	13.1
B	300	1.04	12.9

(19) Moore, A. W. *Chemistry and Physics of Carbon*; Marcel Dekker; New York, 1973; Vol. 11, p 69.

(20) Chung, D. D. L. *J. Mater. Sci.* **1987**, *22*, 4190.

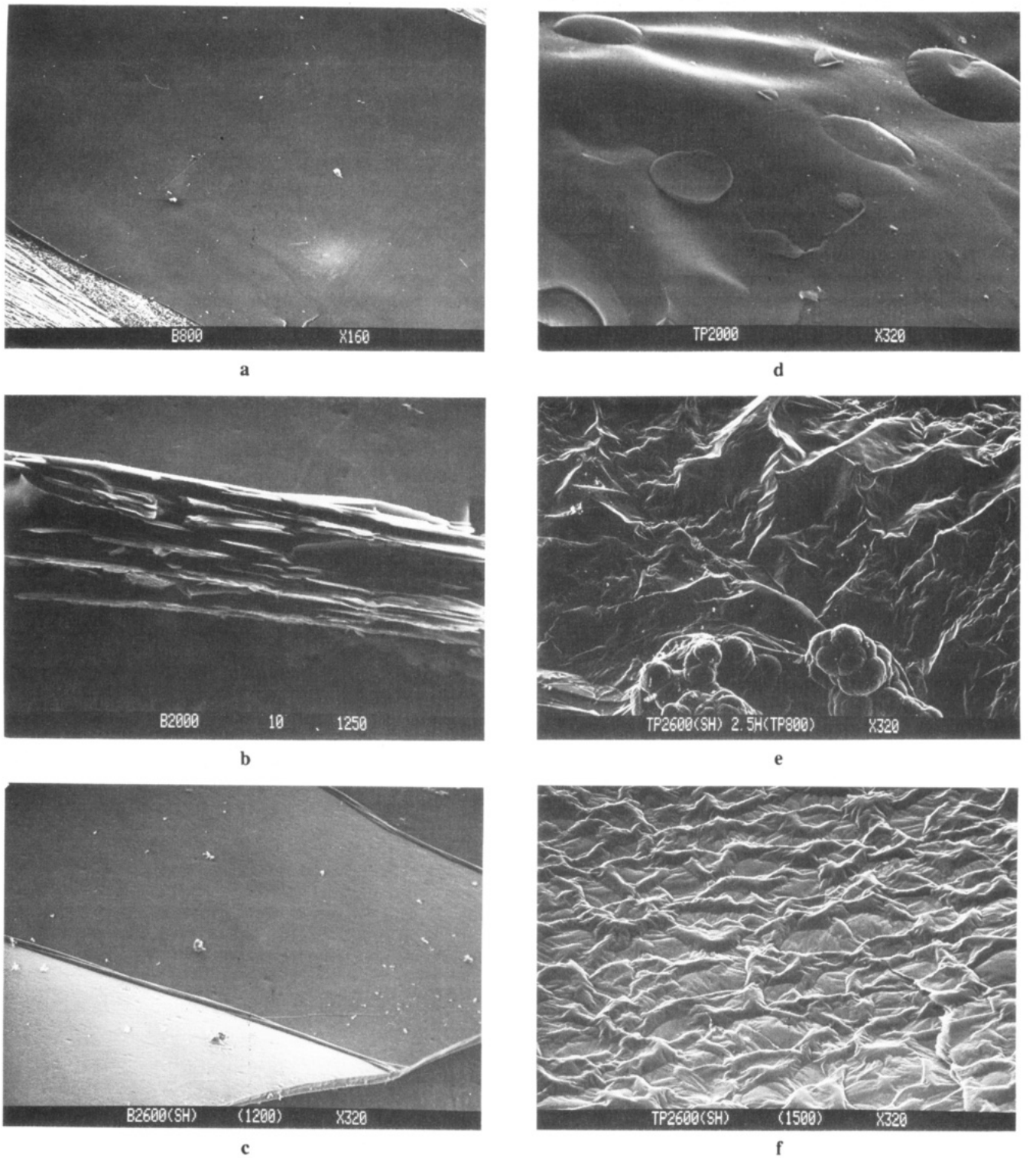

Figure 5. Scanning electron microscopic views of benzene and triphenylene derived graphites: (a) B, 800 °C; (b) edge view of B, 2000 °C; (c) B, 2600 °C, slow heat treatment; (d) TP, 2000 °C; (e) TP, 2600 °C, slow heat treatment showing unusual clusters at bottom of photograph; (f) TP, 2600 °C, slow heat treatment showing highly crinkled surface.

rolysis. Exfoliation is caused from small gas pockets in which the hydrogen and methane are trapped and suddenly released.

Table II is a comparison of ESR measurements on B and TP as-deposited carbon fine powders. The absence of a Dysonian line shape indicates that the particle size is less than the skin depth. Further, the absence of an axial powder pattern indicates that anisotropic orientation has not as yet occurred at 800 °C. ESR absorption can occur as a consequence of both localized spin centers and conduction carriers, producing a single ESR line as a result of exchange mixing of the g values.[21] Spin concentration was determined by comparing the intensity of the sample with that of a reference substance, diphenylpicrylhydrazyl (DPPH).[22] The line width of B(800 °C) is narrower than that of TP (800 °C), decreasing at higher HTT. The line width is related to the spin relaxation time, and differences may relate to the mobilities of electrons in the carbons. The small line width of B (800 °C) is indicative of more

(21) Mrozowski, S. *Carbon* **1988**, *26*, 521.
(22) Mrozowski, S. *Carbon* **1979**, *17*, 227.

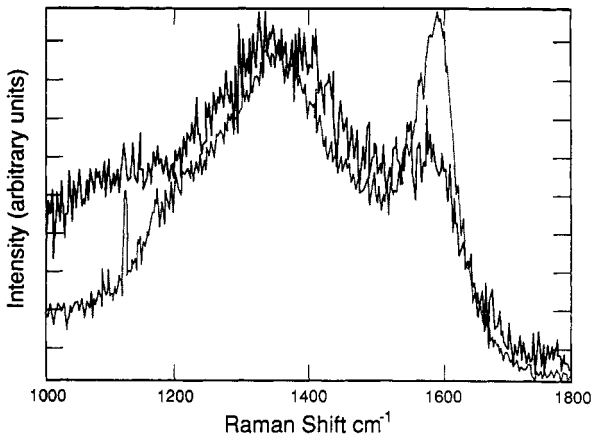

Figure 6. Raman spectra of benzene-(dotted line) and triphenylene- (solid line) derived graphites prepared at 800 °C.

mobile electrons in the more ordered structure. The dependence of line width on temperature for both 800 °C products (Table II) shows a very small activation energy. The spin concentration of B (800 °C) is twice that of TP (800 °C) and probably indicates the greater number of reactive sites per ring in benzene.

A comparison of the Raman spectra of TP and B flakes at 800 °C is given in Figure 6. The ratios of the intensity of the order peak to that of disorder peak are quite different in the two materials, offering additional evidence of the different degree of orientation of the as-deposited carbons. At an HTT of 2600 °C, the disorder peak disappears in all of these samples to yield the conventional graphite Raman spectrum.[23]

Conclusions

The structure of the aromatic hydrocarbon precursor strongly influences the nature of the graphitization process and hence the properties of the resulting graphite. The size and nature of aromatic radicals in the gas phase, their growth prior to nucleation, and the nucleation and growth on substrate are undoubtedly all involved in the process.[24] The larger size of the TP species results in a coarser microstructure with less order at low HTTs, complex morphologies of beaded structures, higher defect densities, and exfoliated regimes at higher HTTs. B-derived radicals appear to be ideal size nucleii, leading to high-quality graphite. Other small aromatics, such as bromobenzene, are also good starting materials for highly ordered graphites.

Acknowledgment. The assistance of Dr. G. Meyer and Dr. P. Heiney with the XRD and W. Shin with the Raman spectra is acknowledged, as well as helpful discussions with Dr. S. Jansen regarding interpretation of the ESR results. This work was supported by the National Science Foundation, Ceramics and Electronic Materials, Division of Materials Research, under Grant No. DMR87-03526. The XRD measurements of P. Heiney were performed using central facilities of the Laboratory for Research on the Structure of Matter, supported by the National Science Foundation Grant No. DMR MRL 88-19885.

Registry No. Benzene, 71-43-2; triphenylene, 217-59-4; graphite, 7782-42-5.

(23) Fischbach, D. B.; Couzi, M. *Carbon* **1986**, *24*, 365.
(24) Kaae, J. L. *Carbon* **1985**, *23*, 665.

Dielectric Response and Conductivity of Poly(propylene oxide) Sodium Polyiodide Complexes. Discussion of Charge Transfer by an Ion Relay Mechanism

Hans-Conrad zur Loye,[†,1] Bruce J. Heyen,[†] Henry O. Marcy,[‡] Donald C. DeGroot,[‡] Carl R. Kannewurf,[‡] and Duward F. Shriver*,[†]

Department of Chemistry and Department of Electrical Engineering and Computer Science, Northwestern University, Evanston, Illinois 60208

Received May 8, 1990

The addition of iodine to poly(propylene oxide), PPO, with or without NaI results in the formation of polyiodides as evidenced by a resonance Raman band at 170 cm^{-1}. The conductivities of these complexes, measured with ac and dc methods, show both ohmic and nonohmic responses characteristic of electronic and ionic conductors, respectively. The conductivity rises with both increasing iodine and salt concentrations. Low-temperature conductivity data showed a very small inflection in the vicinity of T_g for the host polymer, indicating that dynamics of the host polymer are only weakly coupled to the mechanism for conductivity in the polyiodide system. An ion relay along polyiodide chains is consistent with these observations. For comparison purposes, Raman spectra and conductivities were studied for structurally characterized metal compounds containing infinite I_3^- species. In these structures the conductivity is very low, and this is attributed to structural pinning of the polyiodides, which would block ion relay or carrier hopping charge transport.

Introduction

The study of new materials with variable stoichiometry and adjustable electronic properties has led to the discovery of a wealth of chemically interesting dielectric and electrical behavior. Recently, we have explored new polymer materials, polymer salt complexes containing polyiodides, which exhibit both ionic and electronic conductivity. Complexes of the composition $(PEO)_nNaI_x$, where PEO = poly(ethylene oxide), were first studied by

[†] Department of Chemistry.
[‡] Department of Electrical Engineering and Computer Science.

(1) Department of Chemistry, MIT, Cambridge, MA 02139.

0897-4756/90/2802-0603$02.50/0